Pre-Columbian Fire Management Linked to Refractory Black Carbon Emissions in the Amazon

Monica M. Arienzo [1,*], S. Yoshi Maezumi [2,3,4,*], Nathan J. Chellman [1] and Jose Iriarte [4]

[1] Division of Hydrologic Sciences, Desert Research Institution, Reno, NV 89512, USA;
    Nathan.Chellman@dri.edu
[2] Department of Geography and Geology, University of the West Indies Mona, Kingston, Jamaica
[3]   Department of Ecosystem and Landscape Dynamics, University of Amsterdam, 1090 GE Amsterdam,
    The Netherlands
[4] Department of Archaeology, University of Exeter, Exeter EX4 4QE, UK; J.Iriarte@exeter.ac.uk
[*] Correspondence: monica.arienzo@dri.edu (M.M.A.) and s.y.maezumi@uva.nl (S.Y.M.);
    Tel.: +1-775-673-7693 (M.M.A.) and Tel.: +1-876-469-3350 (S.Y.M.)

Abstract: Anthropogenic climate change—combined with increased human-caused ignitions—is leading to increased wildfire frequency, carbon dioxide emissions, and refractory black carbon (rBC) aerosol emissions. This is particularly evident in the Amazon rainforest, where fire activity has been complicated by the synchronicity of natural and anthropogenic drivers of ecological change, coupled with spatial and temporal heterogeneity in past and present land use. One approach to elucidating these factors is through long-term regional fire histories. Using a novel method for rBC determinations, we measured an approximately 3500-year sediment core record from Lake Caranã in the eastern Amazon for rBC influx, a proxy of biomass burning and fossil fuel combustion. Through comparisons with previously published records from Lake Caranã and regional evidence, we distinguished between local and regional rBC emission sources demonstrating increased local emissions of rBC from ~1250 to 500 calendar years before present (cal yr BP), coinciding with increased local-scale fire management during the apex of pre-Columbian activity. This was followed by a regional decline in biomass burning coincident with European contact, pre-Columbian population decline, and regional fire suppression associated with the rubber boom (1850–1910 CE), supporting the minimal influence of climate on regional burning at this time. During the past century, rBC influx has rapidly increased. Our results can serve to validate rBC modeling results, aiding with future predictions of rBC emissions and associated impacts to the climate system.

Keywords: black carbon; macrocharcoal; eastern Amazon; pre-Columbian; fire activity

1. Introduction

Anthropogenic increases in carbon dioxide (CO_2) emissions, combined with an increase in human-caused ignitions, are leading to more severe fire seasons and increasing the frequency of wildfires [1]. This is particularly evident in the Amazon rainforest, the world's largest terrestrial carbon sink [2]. Increased fire activity has the potential to convert Amazon forests from net-carbon sinks to net-carbon sources, with further impacts to the global carbon cycle [3,4].

Refractory black carbon (rBC) aerosols (50–500 nm volume equivalent diameter) are emitted from biomass burning and fossil fuel combustion [5]. Recent work has shown that rBC aerosols have an important role in climate by directly changing Earth's radiation budget [5] and indirectly by changing cloud formation and reducing albedo [6,7]. After CO_2, rBC is the second most important anthropogenic radiative-forcing agent today [5]. Global rBC emissions have increased throughout the

20th century because of continued emissions from fossil fuel combustion and biomass burning (including natural, agricultural, and residential burning) [8,9], with associated climate feedbacks [5]. Continued biomass burning can create positive feedbacks, resulting in increased CO_2 emissions, warmer temperatures, drier forests, increased fire activity, and further loss of forests [10].

Previously, rBC preserved in ice cores [6,11–13], modern lake sediments [14,15], and snow samples [16–19] has been used as a proxy of regional biomass burning and fossil fuel combustion during the past century. These studies demonstrated synchronous variations in rBC emissions with past climate [11,12] and anthropogenic activities associated with industrialization and biomass burning [6,7,15]. Studies in South America have focused on modern rBC deposition in the Andes, an area that provides many people with essential water resources [12,16,17]. These studies have shown that modern rBC deposition was sourced from anthropogenic fossil fuel emissions, as well as biomass burning from the Amazon and nearby residential areas [12,16,17]. Over longer timescales, higher concentrations of rBC were observed during warmer and drier periods, such as the mid-Holocene Climatic Optimum [9000–5000 calendar years before present (cal yr BP)]—while rBC declines during the past 4000 years were attributed to hydroclimatic variations [12]. Osmont et al. [12] also showed that human activities began to play a more prominent role in rBC production during the past 500 years. Recent work also has focused on modern rBC emissions in the Amazon demonstrating a recent increase in rBC emissions associated with biomass burning and industrialization [15,20,21]. To date, however, linkages with rBC emissions and fire activity prior to industrialization [11,12] and linkages with rBC and long-term human emissions [12] and fire management practices remain unclear.

The synchroneity of natural and anthropogenic drivers of ecological change, coupled with the high-degree of spatial and temporal heterogeneity in pre-Columbian land use, make disentangling past natural and anthropogenic fire activity difficult [22–34]. Studies have demonstrated that close examination of the timing of changes across multiple lines of evidence (including local and regional charcoal data, pollen, phytoliths, archaeological, and paleoclimatological data) can aid in disentangling natural and anthropogenic drivers of past fire activity [22–24,35–37]. There is increasing evidence of past fire management in the Amazon as early as the middle Holocene [22,24,37–40], but little is known about how past fire management may have impacted regional-scale biomass burning and subsequent rBC emissions.

While studies have demonstrated a connection between anthropogenic-driven changes in past local-scale (1 m^2 to 10^6 m^2) biomass burning and fire management in the Amazon [41,42], understanding the natural and anthropogenic changes in regional-scale (>10^{10} m^2) biomass burning has been limited because of uncertainties inherent in charcoal-based burning reconstructions arising from variations in regional emission sources [43–49]. Developing a regional-scale record of biomass burning requires numerous, spatially distributed charcoal records. While these charcoal records may come from different kinds of sediment proxy records including macrocharcoal (>50 μm) and pollen slide microcharcoal (<50 μm), such data sets may be influenced by temporal variations in sedimentation, variations in age–depth constraints between records, and low temporal resolution [40,46,50,51]. Furthermore, there are relatively few charcoal records in the Amazon compared to other regions around the world, compounded by a high-degree of habitat heterogeneity and varying pre-Columbian land use histories across lowland Amazonia [22,24–33]. This results in large uncertainties in regional biomass burning reconstructions.

To improve the understanding of natural and anthropogenic sources of rBC emissions on regional scales, we implemented a recently developed, incandescence-based, single-particle method for rBC quantification from Lake Caranã [52]. This method requires a much smaller sample size and is less time-consuming (e.g., it does not require chemical pretreatment), resulting in the potential for relatively high-temporal-resolution records of past rBC deposition compared to previous methods for rBC measurement [52]. Sub-micron rBC particles (50–500 nm volume equivalent diameter) are approximately three orders of magnitude smaller than macrocharcoal fragments (greater than 50 μm [49]; or 125 μm; [45,53]). As a result of the small size, rBC aerosols are transported through aeolian rather than fluvial processes, thus rBC records implicitly reflect regional-scale emissions. This method was applied to a sediment core from Lake Caranã as previous analysis of pollen and

macrocharcoal from the sediment core and other land-use metrics have reconstructed human modification of the landscape throughout the past 4500 years [41,42]. Previous studies of the Lake Caranã record show that fire management, combined with the cultivation of multiple annual crops and the enrichment of edible plants, intensified with increased human populations [41,42]. Of particular interest is the impact of local- and regional-scale fire activity on rBC emissions and the regional ecological impact of land use intensification and fire management in the pre-Columbian period. To test this, we compared rBC influx with macrocharcoal from Lake Caranã [41,42], existing regional charcoal records [41,51], previously published Southern Hemisphere rBC records [11,12], compiled regional archaeological data [41], and paleoclimate data [54] from the eastern Amazon. These data are critical to improving past and future model projections of carbon dynamics and rBC radiative forcing from the Amazon and can be used to inform more effective fire management policies in the 21st century.

2. Materials and Methods

2.1. Study Site

We analyzed rBC in a sediment core recovered from Lake Caranã (02°50′08″S; 55°02′33″W; 5 m above sea level) in the eastern Amazon [41,42] (Figure 1). The lake is ~0.7 km in diameter, ~3 m deep, and located on the fluvial terrace of the eastern bank of Rio Tapajós. Lake Caranã is located within a small closed basin and separated from the main river channel by a sand berm (200 m long, ~ 3-m tall) located on the northeast edge of the lake. The climate is seasonally dry, with a distinct wet season between January and June [41,42]. Today the hydroclimate of the Lake Caranã area of the Amazon Basin is primarily driven by the prevailing easterlies and proximity to the Atlantic coast [54,55]. Considering the atmospheric lifetime for rBC is ~one week [56] and that rBC is primarily deposited through wet deposition [18], the potential regional source area for rBC aerosols is thought to be the eastern Amazon.
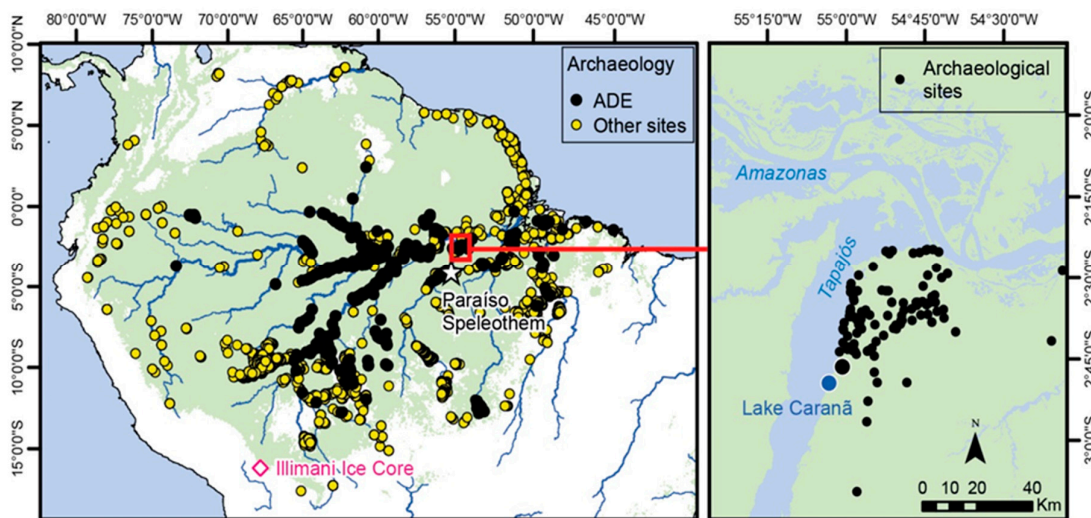

Figure 1. Regional study map. (**Left**) Distribution of archaeological sites including Amazonia dark earths (ADE) used to calculate the Sum of the Calibrated Probability Distributions (SPD) and site frequency values [41,42]. Star indicates Paraíso speleothem record [54]; pink diamond represents Illimani ice core record [12]; red box indicates inset. (**Right**) Study area including Lake Caranã (blue dot). Modified from Maezumi et al. [41,42].

2.2. Age–Depth Model

The age–depth model used in this study was published previously by Maezumi et al. [41,42] and is briefly summarized here. The age–depth model used a combination of ten ^{210}Pb and six Accelerator

Mass Spectrometry (AMS) radiocarbon dates to develop a chronology for Lake Caranã. ^{210}Pb dating was used to constrain the most recent paleo-environmental changes (<250 years), while AMS-radiocarbon dating was used to date sediments older than ~200 years. Ages for the upper Lake Caranã sediment core were modeled using ^{210}Pb radionuclide analyses following standard procedures [57]. The age–depth model was constructed in Bacon v2.2 [58] within R [59] using IntCal13 [42]. Two AMS-radiocarbon dates were identified as potential outliers. Rather than omit these data points, the two outliers were retained and contributed to the uncertainty distribution of the model [42].

2.3. Macrocharcoal

The Lake Caranã sediment core was subsampled for macroscopic charcoal analysis at 0.5 cm intervals from 0 to 210 cm in depth and has been published previously [41,42]. Samples were analyzed for charcoal pieces greater than 125 μm using a modified macroscopic sieving method [45,49,60,61]. Charcoal counts were converted to charcoal influx (the number of charcoal particles cm^{-2} yr^{-1}) and charcoal accumulation rates by dividing by the deposition time (yr cm^{-1}). Charcoal influx data (particles cm^{-2} yr^{-1}) were used as an indicator of fire severity (the amount of biomass consumed during a fire episode or a period of increased burning).

2.4. Sum of the Calibrated Probability Distributions (SPDs) and Site Frequencies

The SPDs are a standard method for representing chronological trends in radiocarbon data sets. SPDs have been shown to be a reliable method to assess past population dynamics in relative terms if an adequate sample size and measures of chronometric hygiene are used [62,63]. See Maezumi et al. [42] for complete methods and the SPD data set. Briefly, SPDs were produced by calibrating each independent date in the sample and adding the results to produce a single density distribution. SPDs were built in OxCal using the sum function and the IntCal13 calibration curve [64,65] with an original data set of 85 radiocarbon dates from the Lower Tapajós. To account for oversampling of some sites and phases within those sites, a 100 year binning procedure was applied [63,66]. The final filtered data set contained 52 dates. The filtered SPD is highly correlated with an SPD built with all radiocarbon dates ($r^2 = 0.991$, P < 0.001). Additionally, a histogram of the number of occupied sites was used as another proxy of human activity based on the medians of the calibrated dates per 200 year intervals.

2.5. Regional Charcoal Curve

Regional charcoal records were compiled from the Global Charcoal Database (GCD, version 2.0) and published records from the eastern Amazon [67]. Charcoal data were analyzed using the paleofire R package software (version 1.1.8) [68]. Eleven charcoal records between 3 °S to 0.2 °N and 43 °W to 54 °W that had greater than 20 charcoal samples were included in this analysis to create a regional composite curve (RCC; Table 1). The sites from the eastern Amazon were selected to provide an average of regional biomass burning during the Holocene. To facilitate inter-site comparison, the eleven records were pretreated using standard protocol [50,51] for transforming and standardizing individual records including (1) transforming non-influx data (e.g., concentration particles cm^{-3}) to influx values (particle cm^{-2} yr^{-1}); (2) homogenizing the variance using the Box-Cox transformation; (3) rescaling the values using a minimax transformation to allow comparisons among sites; and (4) rescaling the values to z-scores using a base period of 200 years. Sites were smoothed with a 200 year, half-width smoothing window and a bootstrap of 100 years [68].

Table 1. Compiled charcoal records used for the regional charcoal curve (RCC) from the eastern Amazon. Records were compiled from the Global Charcoal Database (GCD) [41].

Eastern Amazon	Latitude	Longitude	Reference
Lake Tapera	0.13004	−51.078	[67]
Lake Marcio	0.16377	−51.062	[67]
Lago Caranã	−2.8356	−55.043	[41,42]
Lake Comprida	−1.6249	−54	[69]
Lake Geral	−1.6469	−53.596	[69]
Lago Crispim	−0.6226	−47.644	[70]
Rio Curua	−1.7347	−51.455	[71]
Lagoa da Curuca	−0.7667	−47.85	[72]
Lake Saracuri	−1.6788	−53.57	[73]
Lake Santa Maria	−1.5783	−53.605	[73]
Lago Tapajos	−2.7758	−55.083	[73]

2.6. Refractory Black Carbon

The sediment core was subsampled for rBC at a 0.5 cm resolution between 0 and 102.5 cm in depth. Samples were analyzed at 0.5 cm to be compared with the existing macrocharcoal sample resolution [42]. The subsampled material was dried, followed by homogenization with a Pulverisette planetary mill (Fritsch, Idar-Oberstein, Germany). After grinding, samples were stored in plastic vials until analysis.

Refractory black carbon sample analysis followed the method presented in Chellman et al. [52]. 15 mg of dried and homogenized lake sediment was suspended in 50 mL of ultrapure 18.2 MΩ water in a polypropylene vial. Sediment samples were not chemically pretreated. The weight of both the sediment and water was used to determine the exact ratio of sediment mass to water volume in milligrams of dry sediment per milliliters of water to obtain a final determination of micrograms of rBC per gram sediment. After weighing and suspension, the samples were sonicated (Emerson Electric, St. Louis, MO, USA) and shaken vigorously by hand with the goal of mobilizing rBC from the sediment matrix. The samples were then placed on a platform shaker (Eppendorf, Hamburg, Germany) for 16 h, after which the samples were sonicated again. Prior to analysis, samples were stored in a refrigerator at 10 °C for 24 h.

Aqueous samples, along with any suspended rBC and sediment, were introduced to the analytical system using an autosampler. Samples were filtered through two sequential 20 and 10 μm stainless steel inline filters to remove large suspended sediment particles, diluted with deionized water by a ratio of 11:1 to protect instrumentation and prevent clogging of flow lines. The sample stream was nebulized by an Apex-Q jet-type nebulizer (ESI, Omaha, NE, USA) coupled to an SP2 instrument (Single-Particle Soot Photometer, Droplet Measurement Technologies, Boulder, CO, USA) for rBC quantification. The SP2 instrument has been used extensively for measurement of rBC [6,74,75]. The SP2 was internally calibrated with the manufacturer-specified procedure using the rBC-like material Aquadag to an rBC mass of 100 fg (volume equivalent diameter of ~500 nm). To account for daily changes in efficiency of the sample introduction system, aqueous standards made from the rBC-like material CaboJet 200 were analyzed at the beginning of each day as well as periodically during the day as an external calibration for rBC concentration. The SP2-derived color ratio, an indication of potential interference from iron oxides, indicated no interferences for samples from Lake Caranã.

Replicate measurements were made from a combined and homogenized sample from 70 to 74.5 cm in depth. The average concentration of the combined sample was 1830 ± 538 μg rBC g^{-1} of sediment (mean ± 1σ, n = 22). Concentration measurements (μg rBC g^{-1} of sediment) were converted to rBC influx (μg cm^{-2} yr^{-1}) using sediment accumulation and density measurements.

3. Results

Detailed results of the original paleo-ecological analysis of Lake Caranã can be found in Maezumi et al. [41,42]. Previous analyses include geochemistry (magnetic susceptibility and X-ray fluorescence), pollen, macrocharcoal, and archaeological results [41,42].

Refractory Black Carbon and Macrocharcoal

Refractory black carbon measurements spanned from ~3480 cal yr BP to modern (Figures 2 and 3), with an average sample resolution of ~20 years. To account for variations in the sedimentation rate, rBC influx was calculated (Figure 2, Supplementary Materials). Influx of rBC varied from a maximum of 150 μg cm^{-2} yr^{-1} to a minimum of 3 μg cm^{-2} yr^{-1}. The rBC influx demonstrates good agreement with the existing macrocharcoal influx record [41,42] from Lake Caranã supported by the Pearson's correlation between the rBC and macrocharcoal influx for the entire record (~3480 cal yr BP to modern, r = 0.5, p < 0.0001, n = 170).
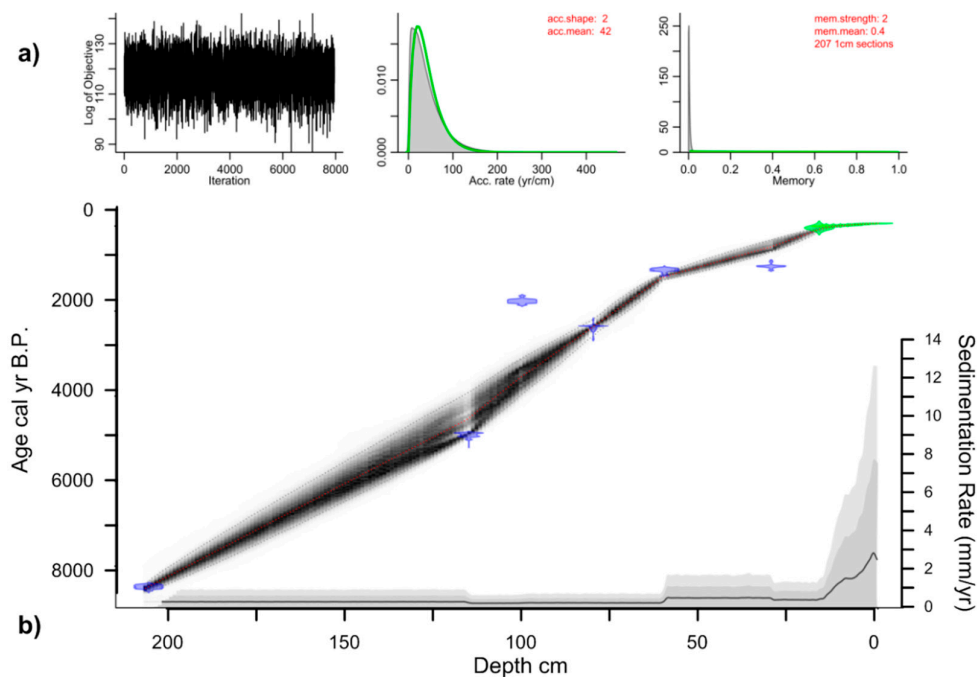

Figure 2. Lake Caranã 210 cm sediment core age–depth model [41,42]. (**a**) Markov chain Monte Carlo iterations from BACON (**top left**) and priors (green curves) and posteriors (gray histograms) for accumulation rate (**top middle**) and memory (**top right**). The age model iterations (black hatching) are based on radiocarbon ages (blue probability density functions) and ^{210}Pb ages (green probability density functions), with model mean (red dashed) and 2σ (black dashed) distributions. (**b**) Accumulation rates from the sediment core. Modified from Maezumi et al. [41,42].

Both the rBC and macrocharcoal influx records indicate low biomass burning from ~3500 to 1200 cal yr BP (Figure 3). The lowest rBC influx values were observed from ~1290 to 1220 cal yr BP, followed by a significant increase in rBC and macrocharcoal influx from ~1200 cal yr BP (Figure 3). Macrocharcoal influx remained elevated and variable until ~500 cal yr BP (Figure 3). Between ~1,100 to 500 cal yr BP, rBC influx showed a slight decline from ~760 to 600 cal yr BP, while the macrocharcoal influx remained elevated (Figure 3). From ~500 to 100 cal yr BP, rBC influx steadily declined by 20-fold with a synchronous decline observed in the macrocharcoal record. This was followed by a 50-fold increase of rBC influx during the last 150 years to maximum rBC values of 150 μg cm^{-2} yr^{-1} in the past decade (Figure 3). We note that while the SP2 is most sensitive to the highly-condensed soot particles created by combustion, it is possible that some of the rBC signal can be attributed to macrocharcoal that has been fragmented into size ranges detectable by the SP2 during

the homogenization process. From the additional assessment of the SP2 data, this is not thought to be a significant contribution to the rBC record.
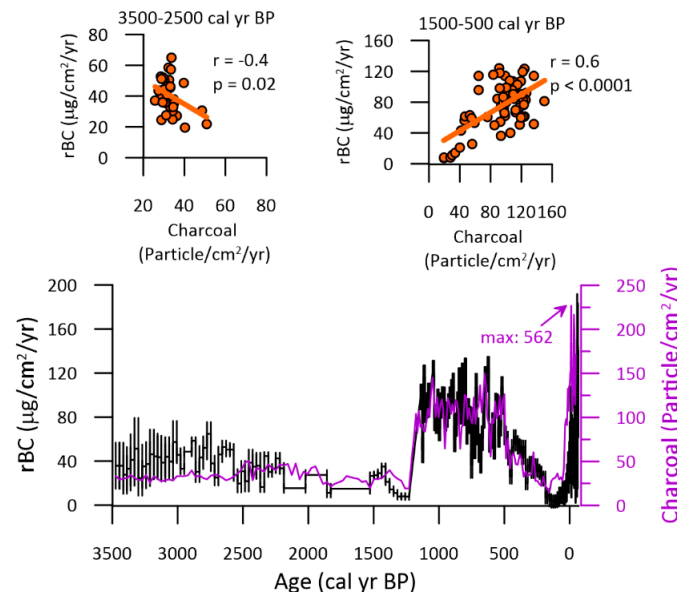

Figure 3. Comparison of macrocharcoal influx (purple) [41,42] and refractory black carbon (rBC) influx (black) from Lake Caranã. Insets show the correlation between macrocharcoal and rBC from 3500 to 2500 cal yr BP (**upper left**) and 1500 to 500 cal yr BP (**upper right**).

4. Discussion

4.1. Local Biomass Burning and rBC Emissions

Previous research indicates that pre-Columbian fire management practices were the dominant driver of fire activity during the late Holocene (after ~3500 cal yr BP) at Lake Caranã [41,42]. The synchronous increase in macrocharcoal data with the SPD values has been previously interpreted [41,42] as an increase in local-scale fire management during the apex of pre-Columbian activity ~1250 to 500 cal yr BP (Figures 1 and 4). Existing taphonomic deposition studies indicate macrocharcoal particles (>125 μm) are thought to be dominated by local-scale biomass burning (1 m² to 10⁶ m²) [45,49,53], whereas the submicron-size fraction of the rBC records was previously thought to reflect regional-scale emissions (>10¹⁰ m²). Satellite based studies demonstrate the potential influence of regional-scale burning on macrocharcoal [76]. However, the good agreement ($r = 0.5$, $p < 0.0001$, $n = 170$) between rBC and macrocharcoal data for the Lake Caranã record (~3480 to present) supports a similar emission source (Figure 3). Based on existing studies, including archaeological data from the area, local-scale fire management is the most likely source of rBC, which likely overwhelmed the regional biomass burning emission sources of rBC.

Interestingly, despite the significant correlation between rBC and macrocharcoal throughout most of the record, there was a negative correlation between the rBC and macrocharcoal records prior to 2500 cal yr BP ($r = -0.4$, $p = 0.02$, $n = 34$) (Figure 3). This was a period characterized by low rBC influx, low macrocharcoal influx, and decreased SPDs (Figure 4). These data suggest an alternative rBC emission source, likely attributed to regional- versus local-scale fire activity prior to 2500 cal yr BP. Alternatively, the intensity of fire (temperature of combustion) at this time may have been different and potentially resulted in the apparent lack of correlation. However, further research is needed to address this hypothesis. From ~1250 to 500 cal yr BP, a positive correlation between rBC influx and macrocharcoal ($r = 0.6$, $p < 0.0001$, $n = 66$) at Lake Caranã was observed, supporting the idea that local biomass burning was the primary source of rBC. The synchronous increase in rBC, macrocharcoal, and SPD values supports the previous interpretation of an increase in local-scale fire management during the apex of pre-Columbian activity (1250 to 500 cal yr BP) [41], suggesting the

dominant role of local-scale fire activity on rBC emissions during this period. In the eastern Amazon, SPD and frequency values declined after ~500 cal yr BP (Figure 4), associated with European contact and colonization (~300 to 30 cal yr BP). The Lake Caranã rBC and macrocharcoal influx show a progressive decline from ~500 to 100 cal yr BP, likely the result of a decline in local pre-Columbian populations [77,78] and subsequent decrease in local-scale fire management practices. The period of record-low biomass burning after ~200 cal yr BP has been attributed to Amazon rubber exploitation and associated fire suppression activity in the eastern Amazon [41].
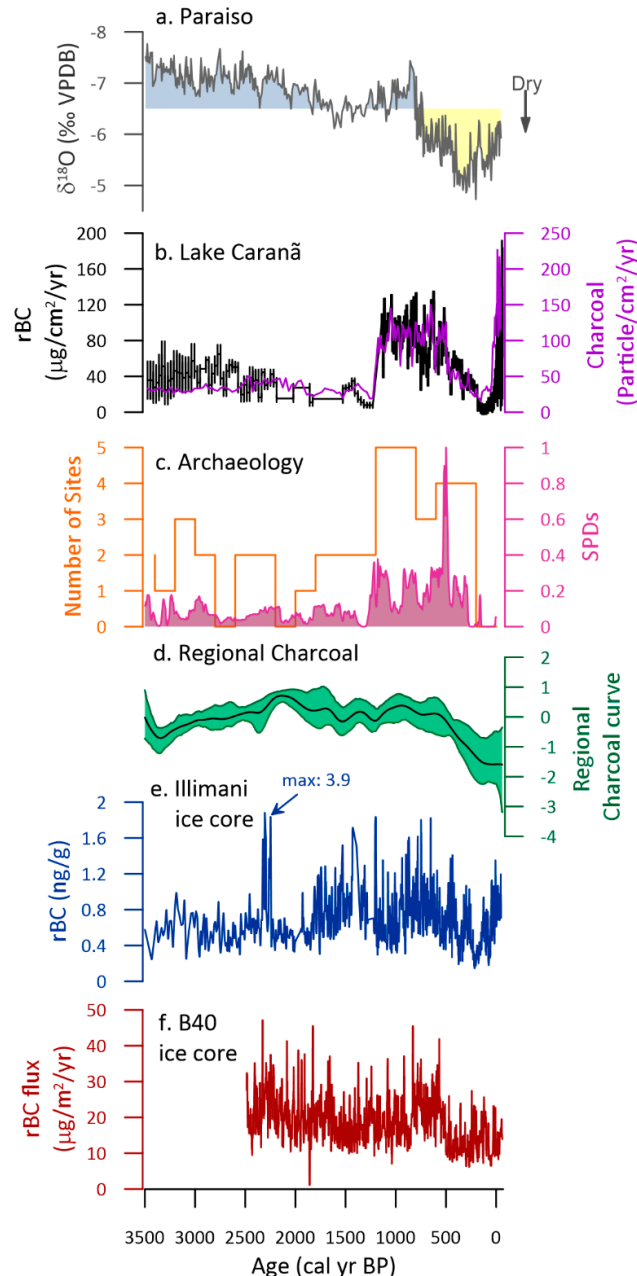

Figure 4. Comparison to regional archives. (**a**) Paraíso speleothem δ¹⁸O values as a proxy of regional hydroclimate from Wang et al. [54]. Increased δ¹⁸O values reflected increased aridity. (**b**) Macrocharcoal [41,42] (purple) and refractory black carbon (rBC) influx (black) from Lake Caranã. (**c**) Archaeology data calculated from the SPDs and site frequency data [42]. (**d**) RCC from the eastern Amazon [41]. (**e**) Illimani ice core rBC concentration (annual averages shown with a 5 year running median) from Osmont et al. [12]. (f) rBC flux from the B40 Antarctic ice core (shown are 7 year medians) from Arienzo et al. [11]. Note—the B40 ice core scale is µg m⁻² yr⁻¹.

4.2. Climate and Biomass Burning

Previous studies have suggested the importance of climate in driving regional-scale fire activity in the Amazon [11,12]. We tested this observation by comparing the Lake Caranã results to the RCC and the regional climate record from the Paraíso Cave speleothem $\delta^{18}O$ values [54]. The Paraíso Cave speleothem $\delta^{18}O$ record has been attributed to variations in precipitation in the eastern Amazon, with $\delta^{18}O$ values negatively correlated with increased precipitation [54] (Figure 4). From ~3500 to 800 cal yr BP, the Paraíso $\delta^{18}O$ record showed a gradual increase in $\delta^{18}O$ values (attributed to decreasing precipitation) synchronous with increased regional biomass burning, as indicated by the RCC values. This was followed by a rapid increase in $\delta^{18}O$ values from ~800 cal yr BP to a peak at ~200 cal yr BP (Figure 4), attributed by a shift to a more arid climate associated with the Little Ice Age (~550 to 250 cal yr BP [79]). This drier climate at ~800 cal yr BP occurred earlier than the decrease in biomass burning indicated by the Lake Caranã rBC and macrocharcoal influx record and the RCC (which declined progressively after ~500 cal yr BP). This supports a minimal influence of climate on local- to regional-biomass burning, particularly after ~500 cal yr BP.

Previous research suggests that the decline in pre-Columbian populations may have played a role in global carbon sequestration at this time. Following European contact in the Americas from ~400 to 30 cal yr BP, widespread collapse of the indigenous populations throughout the Americas occurred [77,78]. The subsequent abandonment of human modified lands and accompanying vegetative regrowth may have sequestered carbon during the 100 years following European arrival [78,80,81]. The synchronicity of the rBC, macrocharcoal, and RCC decrease in the eastern Amazon after ~500 cal yr BP, despite climate conditions drier than present, suggests the dominant role of pre-Columbian fire management in local- and regional-scale biomass burning. The observed decline in rBC emissions associated with pre-Columbian population collapse and the cessation of local-scale fire management practices may have had an additional climate impact, but further research is needed on the role of reduced rBC emissions to the climate system.

Two recently published Southern Hemisphere rBC records demonstrate a decline associated with the Little Ice Age that has been previously attributed to South American hydroclimatic shifts [11,12]. Considering identification of the dominant role of pre-Columbian fire management in local- and regional-scale biomass burning, we compared Lake Caranã rBC, macrocharcoal influx, and the RCC to these previously published records (Figure 4). The rBC ice core record from the Illimani glacier (Figure 1) was previously interpreted as sourced from regional Amazon biomass burning and local (Altiplano) biomass burning [12], and the B40 ice core in eastern Antarctica was previously interpreted as a distal proxy for biomass burning sourced from a much larger region of South America, including the eastern Amazon and the Pampas region to the south [11]. We included the distal records of Illimani and B40 as they are the only other rBC records from the Southern Hemisphere. In addition, previous research [11] suggests the B40 rBC ice core record was, in part, sourced from the eastern Amazon, therefore allowing a comparison to a rBC record from the source region. The decline in rBC and macrocharcoal influx at Lake Caranã and the RCC values at ~500 cal yr BP were synchronous with the Illimani rBC concentration decline (Figure 4). The steady decline in rBC observed in the Illimani ice core was interrupted by two notable increases. One rBC concentration increase occurred during the apex of the Inca Empire (490 to 400 cal yr BP) and a second increase later (320 to 280 cal yr BP), which was associated with increased colonial (silver extraction) mining in the Andes [12,82,83] supporting the importance of local Andean anthropogenic emissions in the Illimani ice core rBC record. Similar to the Lake Caranã and Illimani ice core record, the B40 ice core in Antarctica exhibited low rBC flux after ~500 cal yr BP, but the decline at ~500 yr BP was more gradual in Lake Caranã than in the B40 ice core (Figure 4). This difference was potentially the result of the distal nature of the ice core site and the much greater rBC source area [11]. Therefore, long-range transport and atmospheric mixing likely affected the rBC record from the B40 site. We hypothesize that the rBC decline observed in the Illimani and B40 records associated with the Little Ice Age may have, in part, been impacted by the decline in pre-Columbian populations throughout South America [77,78] and subsequent decrease in local- to regional-scale fire management practices.

4.4. Modern Black Carbon Emission Sources

A 50-fold increase of rBC influx observed during the last 150 years from Lake Caranã was synchronous with the macrocharcoal data (Figure 5). The recent increase in macrocharcoal was shown to be related to increases in fire severity in the area surrounding Lake Caranã because of historic fire suppression, resulting in fuel build-up, and anthropogenic climate change. Recent warmer and drier climates have created conditions optimal for wildfire activity in the eastern Amazon [2,41]. As modern rBC is sourced from biomass burning and fossil fuels, differences between the macrocharcoal and rBC record may be caused by source variations. A comparison to emission inventories for the Amazon would aid with assessment of modern rBC sources, but very few regional estimates for South American rBC emissions have been conducted [84]. As an alternative, we compared rBC influx measurements to global emission inventories [5,9,85] to assess potential emission sources of modern rBC.
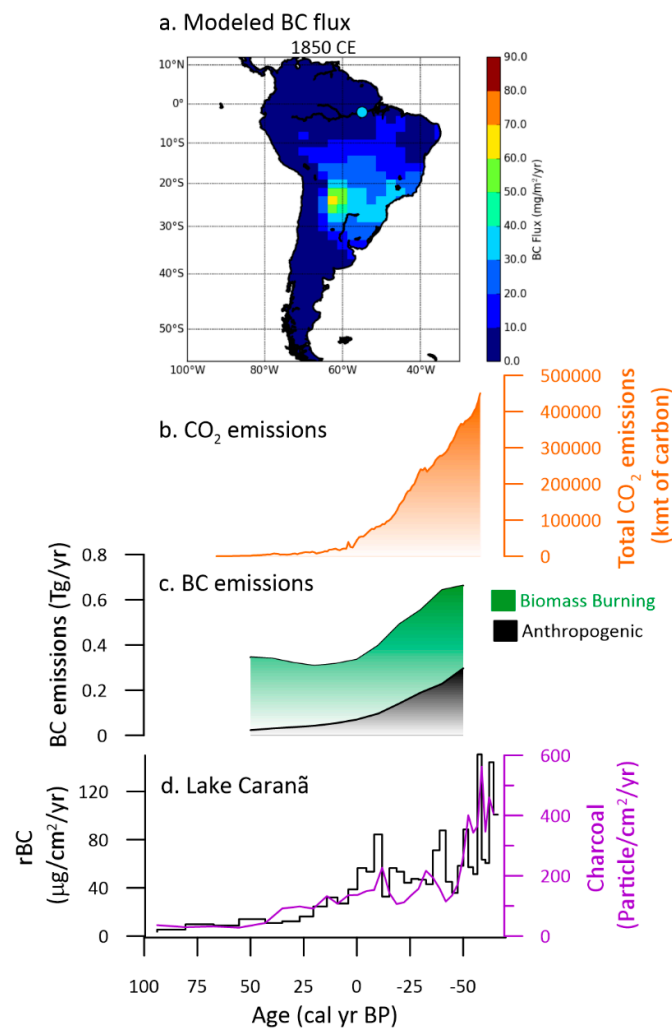

Figure 5. Recent indicators of biomass burning and anthropogenic emissions. (**a**) Black Carbon (BC) model results from Lee et al. [85] for 1850 CE (BC flux in mg m^{-2} yr^{-1}) compared to rBC influx from Lake Caranã shown in the circle. (**b**) Total fossil fuel CO_2 emissions from Central America, South America, and Caribbean nations [86]. (**c**) Stacked area chart of Southern Hemisphere South America BC emissions from anthropogenic sources (black) and biomass burning (green) [9]. (**d**) Macrocharcoal (purple) [41] and refractory BC influx (black) from Lake Caranã.

The measured rBC influx from Lake Caranã was greater than the modeled BC depositional flux for 1850 CE proposed by Lee et al. [85] (Figure 5a). The modeled BC flux was developed based on

existing estimates from the high latitudes, with a majority of the records used to evaluate the model from the Northern Hemisphere [85]. The BC depositional flux model has not been evaluated against any low-latitude records from the Southern Hemisphere [85] and, therefore, may be offset from the rBC observations from Lake Caranã.

Since the 1900s, South and Central America have undergone rapid industrialization, resulting in increased fossil fuel emissions (Figure 5b). Modeling of BC emissions from South American biomass burning and anthropogenic sources suggests that both emission sources increased from 1950 to 1990 CE because of deforestation and industrialization (Figure 5c) [9,84]. Emission estimates from 1900 to 2000 CE show that biomass burning was the greater source of rBC aerosols (Figure 5c). For the year 2000 CE, ~55 to 65% of BC emissions were sourced from the burning of forests and grasses [5,9]. Considering the modeled emission estimates and positive correlation between rBC influx and macrocharcoal for Lake Caranã (r = 0.8, p < 0.0001, n = 33) from 1870 to 2014 CE, the primary source of rBC at Lake Caranã was most likely recent increases in biomass burning rather than fossil fuel emissions.

Using a method requiring significant chemical pre-treatment and analysis by a carbon analyzer, Cordeiro et al. [15] analyzed a sediment core from the Amazon. The sediment core was collected south of Lake Caranã in the Alta Floresta region of the state of Mato Grosso, central Brazil and was dated to 1978 CE [15]. Results show a range from 600 to 8800 µg cm^{-2} yr^{-1} from 1978 to 1996 CE [15], much greater than the rBC influx variations observed in Lake Caranã for the same time period. Discrepancies between these data suggest additional lake sediment rBC records from the low-latitude South America region are needed.

4.5. Future Implications for rBC Production

Our rBC record from Lake Caranã has important implications for the long-term role of human-driven fire activity on rBC emissions. The strong correlation between the macrocharcoal and rBC data suggests that the burning of local biomass strongly influences rBC in lake sediments proximal to emission sources both currently and in the past. Today, rBC emissions are compounded by anthropogenic climate change, which is increasing the frequency and severity of droughts in the Amazon [10], resulting in more frequent and severe wildfires in this region [2]. These factors can contribute to positive feedbacks that threaten to convert the Amazon from a net-carbon sink to a net-carbon source, further impacting the global carbon budget [87]. In addition, under increased CO_2 emission scenarios, climate model experiments demonstrate the Amazon Basin will likely experience substantial declines in regional-scale annual rainfall [88], coupled with increased occurrence of climate extremes [89]. Fire modeling of Amazon understory projects an increase in fire frequency and duration under increased carbon emission scenarios [90]. Future projections also indicate rBC emissions will continue to increase from South American biomass burning, compounded by fossil fuel emissions from transportation with broader implications for rBC climate forcing [5]. Therefore, factoring in the important role humans play in the production of rBC via human-caused wildfires, anthropogenic climate change, and industrialization should be addressed in future management, fire modeling, and climate modeling scenarios.

5. Conclusions

The incandescence-based, single-particle method [52] for rBC determinations requires a much smaller sample size (0.015 g in this study) and is less time-consuming (e.g., it does not require chemical pretreatment) when compared to previous methods for rBC measurement. Our results demonstrate the applicability of this new method for reconstructing rBC in low latitude sites an area of few long-term studies [12,15].

Previous research conducted on rBC in distal ice cores suggests that rBC represents regional, long-distance transport of biomass burning and fossil fuel emissions. Our research demonstrates the important role of local- to regional-scale fire management on records of rBC proximal to emission sources. Through comparisons with previously published macrocharcoal records from Lake Caranã, existing paleofire proxies, and regional archaeological evidence, we distinguished between local and

regional rBC emission sources demonstrating increased local emissions of rBC from ~1250 to 500 cal yr BP coincident with increased local-scale fire management during the apex of pre-Columbian activity. This was followed by a regional decline in biomass burning coincident with European contact, pre-Columbian population decline, and regional fire suppression, which is reflected in rBC records from South America and Antarctica. These results can serve to validate rBC modeling results (e.g., [9,85,91]) important for understanding radiative forcing and global climate feedback.

References

1. Costafreda-Aumedes, S.; Comas, C.; Vega-Garcia, C. Human-caused fire occurrence modelling in perspective: A review. *Int. J. Wildl. Fire* **2017**, *26*, 983–998, doi:10.1071/WF17026.
2. Aragao, L.; Anderson, L.; Fonseca, M.; Rosan, T.; Vedovato, L.; Wagner, F.; Silva, C.; Silva, C.; Arai, E.; Aguiar, A.; et al. 21st Century drought-related fires counteract the decline of Amazon deforestation carbon emissions. *Nature Commun.* **2018**, *9*, doi:10.1038/s41467-017-02771-y.
3. Baccini, A.; Walker, W.; Carvalho, L.; Farina, M.; Sulla-Menashe, D.; Houghton, R. Tropical forests are a net carbon source based on aboveground measurements of gain and loss. *Science* **2017**, *358*, 230–233, doi:10.1126/science.aam5962.
4. De Faria, B.; Brando, P.; Macedo, M.; Panday, P.; Soares, B.; Coe, M. Current and future patterns of fire-induced forest degradation in Amazonia. *Environ. Res. Lett.* **2017**, *12*, doi:10.1088/1748-9326/aa69ce.
5. Bond, T.; Doherty, S.; Fahey, D.; Forster, P.; Berntsen, T.; DeAngelo, B.; Flanner, M.; Ghan, S.; Karcher, B.; Koch, D.; et al. Bounding the role of black carbon in the climate system: A scientific assessment. *J. Geophys. Res.-Atmos.* **2013**, *118*, 5380–5552, doi:10.1002/jgrd.50171.
6. McConnell, J.; Edwards, R.; Kok, G.; Flanner, M.; Zender, C.; Saltzman, E.; Banta, J.; Pasteris, D.; Carter, M.; Kahl, J. 20th-century industrial black carbon emissions altered Arctic climate forcing. *Science* **2007**, *317*, 1381–1384, doi:10.1126/science.1144856.
7. Painter, T.; Flanner, M.; Kaser, G.; Marzeion, B.; VanCuren, R.; Abdalati, W. End of the Little Ice Age in the Alps forced by industrial black carbon. *Proc. Natl. Acad. Sci. USA* **2013**, *110*, 15216–15221, doi:10.1073/pnas.1302570110.
8. Bond, T.; Bhardwaj, E.; Dong, R.; Jogani, R.; Jung, S.; Roden, C.; Streets, D.; Trautmann, N. Historical emissions of black and organic carbon aerosol from energy-related combustion, 1850-2000. *Glob. Biogeochem. Cy.* **2007**, *21*, doi:10.1029/2006GB002840.
9. Lamarque, J.; Bond, T.; Eyring, V.; Granier, C.; Heil, A.; Klimont, Z.; Lee, D.; Liousse, C.; Mieville, A.; Owen, B.; et al. Historical (1850-2000) gridded anthropogenic and biomass burning emissions of reactive gases and aerosols: Methodology and application. *Atmos. Chem. Phys.* **2010**, *10*, 7017–7039, doi:10.5194/acp-10-7017-2010.
10. IPCC. Part A: Global and Sectoral Aspects: Working Group II Contribution to the IPCC Fifth Assessment Report. In *Climate Change 2014 – Impacts, Adaptation and Vulnerability: Volume 1: Global and Sectoral Aspects*; Intergovernmental Panel on Climate, C., Ed.; Cambridge University Press: Cambridge, UK, 2014; Vol. 1, pp. i-ii.

11. Arienzo, M.; McConnell, J.; Murphy, L.; Chellman, N.; Das, S.; Kipfstuhl, S.; Mulvaney, R. Holocene black carbon in Antarctica paralleled Southern Hemisphere climate. *J. Geophys. Res.-Atmos.* **2017**, *122*, 6713–6728, doi:10.1002/2017JD026599.

12. Osmont, D.; Sigl, M.; Eichler, A.; Jenk, T.M.; Schwikowski, M. A Holocene black carbon ice-core record of biomass burning in the Amazon Basin from Illimani, Bolivia. *Climate of the Past* **2019**, *15*, 579–592, doi:10.5194/cp-15-579-2019.

13. Zennaro, P.; Kehrwald, N.; McConnell, J.R.; Schuepbach, S.; Maselli, O.J.; Marlon, J.; Vallelonga, P.; Leuenberger, D.; Zangrando, R.; Spolaor, A.; et al. Fire in ice: Two millennia of boreal forest fire history from the Greenland NEEM ice core. *Climate of the Past* **2014**, *10*, 1905–1924, doi:10.5194/cp-10-1905-2014.

14. Han, Y.M.; Cao, J.J.; Yan, B.Z.; Kenna, T.C.; Jin, Z.D.; Cheng, Y.; Chow, J.C.; An, Z.S. Comparison of elemental carbon in lake sediments measured by three different methods and 150-year pollution history in eastern China. *Environ. Sci. Technol.* **2011**, *45*, 5287–5293, doi:10.1021/es103518c.

15. Cordeiro, R.; Turcq, B.; Ribeiro, M.; Lacerda, L.; Capitaneo, J.; da Silva, A.; Sifeddine, A.; Turcq, P. Forest fire indicators and mercury deposition in an intense land use change region in the Brazilian Amazon (Alta Floresta, MT). *Sci. Total Environ.* **2002**, *293*, 247–256, doi:10.1016/S0048-9697(02)00045-1.

16. Schmitt, C.; All, J.; Schwarz, J.; Arnott, W.; Cole, R.; Lapham, E.; Celestian, A. Measurements of light-absorbing particles on the glaciers in the Cordillera Blanca, Peru. *Cryosphere* **2015**, *9*, 331–340, doi:10.5194/tc-9-331-2015.

17. Rowe, P.M.; Cordero, R.R.; Warren, S.G.; Stewart, E.; Doherty, S.J.; Pankow, A.; Schrempf, M.; Casassa, G.; Carrasco, J.; Pizarro, J.; et al. Black carbon and other light-absorbing impurities in snow in the Chilean Andes. *Sci. Rep.* **2019**, *9*, 4008, doi:10.1038/s41598-019-39312-0.

18. Flanner, M.; Zender, C.; Randerson, J.; Rasch, P. Present-day climate forcing and response from black carbon in snow. *J. Geophys. Res.-Atmos.* **2007**, *112*, doi:10.1029/2006JD008003.

19. Macdonald, K.; Sharma, S.; Toom, D.; Chivulescu, A.; Platt, A.; Elsasser, M.; Huang, L.; Leaitch, R.; Chellman, N.; McConnell, J.; et al. Temporally delineated sources of major chemical species in high Arctic snow. *Atmos. Chem. Phys.* **2018**, *18*, 3485–3503, doi:10.5194/acp-18-3485-2018.

20. Evangelista, H.; Maldonado, J.; Godoi, R.; Pereira, E.; Koch, D.; Tanizaki-Fonseca, K.; Van Grieken, R.; Sampaio, M.; Setzer, A.; Alencar, A.; et al. Sources and transport of urban and biomass burning aerosol black carbon at the South-West Atlantic coast. *J. Atmos. Chem.* **2007**, *56*, 225–238.

21. Artaxo, P.; Fernandes, E.; Martins, J.; Yamasoe, M.; Hobbs, P.; Maenhaut, W.; Longo, K.; Castanho, A. Large-scale aerosol source apportionment in Amazonia. *J. Geophys. Res.-Atmos.* **1998**, *103*, 31837–31847, doi:10.1029/98JD02346.

22. Maezumi, S.; Whitney, B.; Mayle, F.; de Souza, J.; Iriarte, J. Reassessing climate and pre-Columbian drivers of paleofire activity in the Bolivian Amazon. *Quaternary Int.* **2018**, *488*, 81–94, doi:10.1016/j.quaint.2017.11.053.

23. McMichael, C.; Feeley, K.; Dick, C.; Piperno, D.; Bush, M. Comment on "Persistent effects of pre-Columbian plant domestication on Amazonian forest composition". *Science* **2017**, *358*, doi:10.1126/science.aan8347.

24. McMichael, C.N.H.; Bush, M.B. Spatiotemporal patterns of pre-Columbian people in Amazonia. *Quaternary Res.* **2019**, 1-17.

25. Bush, M.; Silman, M.; Listopad, C. A regional study of Holocene climate change and human occupation in Peruvian Amazonia. *J. Biogeogr.* **2007**, *34*, 1342–1356, doi:10.1111/j.1365-2699.2007.01704.x.

26. Iriarte, J.; Power, M.; Rostain, S.; Mayle, F.; Jones, H.; Watling, J.; Whitney, B.; Mckey, D. Fire-free land use in pre-1492 Amazonian savannas. *Proc. Natl. Acad. Sci. USA* **2012**, *109*, 6473–6478, doi:10.1073/pnas.1201461109.

27. Carson, J.; Whitney, B.; Mayle, F.; Iriarte, J.; Prumers, H.; Soto, J.; Watling, J. Environmental impact of geometric earthwork construction in pre-Columbian Amazonia. *Proc. Natl. Acad. Sci. USA* **2014**, *111*, 10497–10502, doi:10.1073/pnas.1321770111.

28. Mayle, F.; Iriarte, J. Integrated palaeoecology and archaeology - a powerful approach for understanding pre-Columbian Amazonia. *J. Archaeol. Sci.* **2014**, *51*, 54–64, doi:10.1016/j.jas.2012.08.038.

29. McMichael, C.; Piperno, D.; Bush, M.; Silman, M.; Zimmerman, A.; Raczka, M.; Lobato, L. Sparse Pre-Columbian Human Habitation in Western Amazonia. *Science* **2012**, *336*, 1429–1431, doi:10.1126/science.1219982.

30. Piperno, D.R. *Phytoliths: A Comprehensive Guide for Archaeologists and Paleoecologists*; Rowman Altamira: Lanham, MD, USA, 2006.

31. Clement, C.; Cristo-Araújo, D.; Coppens D'Eeckenbrugge, G.; Alves Pereira, A.; Picanço-Rodrigues, D. Origin and domestication of native Amazonian crops. *Diversity* **2010**, *2*, 72–106.

32. Thomas, E.; Alcázar Caicedo, C.; McMichael, C.H.; Corvera, R.; Loo, J. Uncovering spatial patterns in the natural and human history of Brazil nut (Bertholletia excelsa) across the Amazon Basin. *J. Biogeogr.* **2015**, *42*, 1367–1382.

33. Whitney, B.S.; Dickau, R.; Mayle, F.E.; Walker, J.H.; Soto, J.D.; Iriarte, J. Pre-Columbian raised-field agriculture and land use in the Bolivian Amazon. *The Holocene* **2014**, *24*, 231–241.

34. Bush, M.; McMichael, C.; Piperno, D.; Silman, M.; Barlow, J.; Peres, C.; Power, M.; Palace, M. Anthropogenic influence on Amazonian forests in pre-history: An ecological perspective. *J. Biogeogr.* **2015**, *42*, 2277–2288, doi:10.1111/jbi.12638.

35. Urrego, D.; Bush, M.; Silman, M.; Niccum, B.; De La Rosa, P.; McMichael, C.; Hagen, S.; Palace, M. Holocene fires, forest stability and human occupation in south-western Amazonia. *J. Biogeogr.* **2013**, *40*, 521–533, doi:10.1111/jbi.12016.

36. Loughlin, N.; Gosling, W.; Mothes, P.; Montoya, E. Ecological consequences of post-Columbian indigenous depopulation in the Andean-Amazonian corridor. *Nature Ecol. Evol.* **2018**, *2*, 1233–1236, doi:10.1038/s41559-018-0602-7.

37. Bush, M.; Correa-Metrio, A.; McMichael, C.; Sully, S.; Shadik, C.; Valencia, B.; Guilderson, T.; Steinitz-Kannan, M.; Overpeck, J. A 6900-year history of landscape modification by humans in lowland Amazonia. *Quaternary Sci. Rev.* **2016**, *141*, 52–64, doi:10.1016/j.quascirev.2016.03.022.

38. Watling, J.; Iriarte, J.; Mayle, F.; Schaan, D.; Pessenda, L.; Loader, N.; Street-Perrott, F.; Dickau, R.; Damasceno, A.; Ranzi, A. Impact of pre-Columbian "geoglyph" builders on Amazonian forests. *Proc. Natl. Acad. Sci. USA* **2017**, *114*, 1868–1873, doi:10.1073/pnas.1614359114.

39. Brugger, S.; Gobet, E.; van Leeuwen, J.; Ledru, M.; Colombaroli, D.; van der Knaap, W.; Lombardo, U.; Escobar-Torrez, K.; Finsinger, W.; Rodrigues, L.; et al. Long-term man-environment interactions in the Bolivian Amazon: 8000 years of vegetation dynamics. *Quaternary Sci. Rev.* **2016**, *132*, 114–128, doi:10.1016/j.quascirev.2015.11.001.

40. Irion, G.; Bush, M.; de Mello, J.; Stuben, D.; Neumann, T.; Muller, G.; De, J.; Junk, J. A multiproxy palaeoecological record of Holocene lake sediments from the Rio Tapajos, eastern Amazonia. *Palaeogeogr. Palaeoclimatol. Palaeoecol.* **2006**, *240*, 523–535, doi:10.1016/j.palaeo.2006.03.005.

41. Maezumi, S.; Robinson, M.; de Souza, J.; Urrego, D.; Schaan, D.; Alves, D.; Iriarte, J. New Insights From Pre-Columbian Land Use and Fire Management in Amazonian Dark Earth Forests. *Front. Ecol. Evol.* **2018**, *6*, doi:10.3389/fevo.2018.00111.

42. Maezumi, S.; Alves, D.; Robinson, M.; de Souza, J.; Levis, C.; Barnett, R.; de Oliveira, E.; Urrego, D.; Schaan, D.; Iriarte, J. The legacy of 4,500 years of polyculture agroforestry in the eastern Amazon. *Nature Plants* **2018**, *4*, 540–547, doi:10.1038/s41477-018-0205-y.

43. Higuera, P.; Peters, M.; Brubaker, L.; Gavin, D. Understanding the origin and analysis of sediment-charcoal records with a simulation model. *Quaternary Sci. Rev.* **2007**, *26*, 1790–1809, doi:10.1016/j.quascirev.2007.03.010.

44. Peters, M.; Higuera, P. Quantifying the source area of macroscopic charcoal with a particle dispersal model. *Quaternary Res.* **2007**, *67*, 304–310, doi:10.1016/j.yqres.2006.10.004.

45. Brown, K.J.; Power, M.J. Charred particle analyses. In *The Encyclopedia of Quaternary Science*; Elias, S.A., Ed.; Elsevier: Amsterdam, The Netherlands. 2013; Volume 2; pp. 716-729.

46. Marlon, J.; Bartlein, P.J.; Daniau, A.-L.; Harrison, S.P.; Maezumi, S.Y.; Power, M.J.; Tinner, W.; Vanniere, B. Global biomass burning: A synthesis and review of Holocene paleofire records and their controls. *Quaternary Sci. Rev.* **2013**, *65*, 5–25, doi:10.1016/j.quascirev.2012.11.029.

47. Power, M.; Marlon, J.; Bartlein, P.; Harrison, S. Fire history and the Global Charcoal Database: A new tool for hypothesis testing and data exploration. *Palaeogeogr. Palaeoclimatol. Palaeoecol.* **2010**, *291*, 52–59, doi:10.1016/j.palaeo.2009.09.014.

48. Power, M.J.; Bush, M.B.; Behling, H.; Horn, S.P.; Mayle, F.E.; Urrego, D.H. Paleofire activity in tropical America during the last 21 ka: A regional synthesis based on sedimentary charcoal. *PAGES Newsl.* **2010**, *18*, 73–75.

49. Whitlock, C.; Larsen, C. Charcoal as a fire proxy. In *Tracking Environmental Change Using Lake Sediments*, Last, W.M., Smol, J.P. Eds. Springer: Dordrecht, The Netherlands, 2002; pp. 75–97.

50. Marlon, J.; Bartlein, P.J.; Carcaillet, C.; Gavin, D.G.; Harrison, S.P.; Higuera, P.E.; Joos, F.; Power, M.J.; Prentice, I.C. Climate and human influences on global biomass burning over the past two millennia. *Nature Geosci.* **2008**, *1*, 697–702, doi:10.1038/ngeo313.

51. Power, M.J.; Marlon, J.; Ortiz, N.; Bartlein, P.J.; Harrison, S.P.; Mayle, F.E.; Ballouche, A.; Bradshaw, R.H.W.; Carcaillet, C.; Cordova, C.; et al. Changes in fire regimes since the Last Glacial Maximum: an assessment based on a global synthesis and analysis of charcoal data. *Clim. Dyn.* **2008**, *30*, 887–907, doi:10.1007/s00382-007-0334-x.

52. Chellman, N.; McConnell, J.; Heyvaert, A.; Vanniere, B.; Arienzo, M.; Wennrich, V. Incandescence-based single-particle method for black carbon quantification in lake sediment cores. *Limnol. Oceanogr.-Methods* **2018**, *16*, 711–721, doi:10.1002/lom3.10276.

53. Leys, B.; Brewer, S.C.; McConaghy, S.; Mueller, J.; McLauchlan, K.K. Fire history reconstruction in grassland ecosystems: amount of charcoal reflects local area burned. *Environ. Res. Lett.* **2015**, *10*, 114009.

54. Wang, X.; Edwards, R.; Auler, A.; Cheng, H.; Kong, X.; Wang, Y.; Cruz, F.; Dorale, J.; Chiang, H. Hydroclimate changes across the Amazon lowlands over the past 45,000 years. *Nature* **2017**, *541*, 204–+, doi:10.1038/nature20787.

55. Vuille, M.; Werner, M. Stable isotopes in precipitation recording South American summer monsoon and ENSO variability: observations and model results. *Clim. Dyn.* **2005**, *25*, 401–413, doi:10.1007/s00382-005-0049-9.

56. Ramanathan, V.; Carmichael, G. Global and regional climate changes due to black carbon. *Nature Geosci.* **2008**, *1*, 221–227, doi:10.1038/ngeo156.

57. Appleby, P.G. Chronostratigraphic techniques in recent sediments. In *Tracking Environmental Change Using Lake Sediments*, Last, W.M., Smol, J.P. Eds. Springer: Dordrecht, The Netherlands, 2002; pp. 171–203.

58. Blaauw, M.; Christen, J.; Mauquoy, D.; van der Plicht, J.; Bennett, K. Testing the timing of radiocarbon-dated events between proxy archives. The *Holocene* **2007**, *17*, 283–288, doi:10.1177/0959683607075857.

59. R Core Team. *R: A Language and Environment for Statistical Computing*; R Core Team: Vienna, Austria, 2013.

60. Jensen, K.; Lynch, E.; Calcote, R.; Hotchkiss, S. Interpretation of charcoal morphotypes in sediments from Ferry Lake, Wisconsin, USA: do different plant fuel sources produce distinctive charcoal morphotypes? *Holocene* **2007**, *17*, 907–915, doi:10.1177/0959683607082405.

61. Tweiten, M.; Hotchkiss, S.; Booth, R.; Calcote, R.; Lynch, E. The response of a jack pine forest to late-Holocene climate variability in northwestern Wisconsin. *Holocene* **2009**, *19*, 1049–1061, doi:10.1177/0959683609340993.

62. Shennan, S.; Downey, S.; Timpson, A.; Edinborough, K.; Colledge, S.; Kerig, T.; Manning, K.; Thomas, M. Regional population collapse followed initial agriculture booms in mid-Holocene Europe. *Nature Commun.* **2013**, *4*, doi:10.1038/ncomms3486.

63. Timpson, A.; Colledge, S.; Crema, E.; Edinborough, K.; Kerig, T.; Manning, K.; Thomas, M.; Shennan, S. Reconstructing regional population fluctuations in the European Neolithic using radiocarbon dates: a new case-study using an improved method. *J. Archaeol. Sci.* **2014**, *52*, 549–557, doi:10.1016/j.jas.2014.08.011.

64. Reimer, P.J.; Bard, E.; Bayliss, A.; Beck, J.W.; Blackwell, P.G.; Ramsey, C.B.; Buck, C.E.; Cheng, H.; Edwards, R.L.; Friedrich, M. IntCal13 and Marine13 radiocarbon age calibration curves 0–50,000 years cal BP. *Radiocarbon* **2013**, *55*, 1869–1887.

65. Ramsey, C.B.; Lee, S. Recent and planned developments of the program OxCal. *Radiocarbon* **2013**, *55*, 720–730.

66. Goldberg, A.; Mychajliw, A.; Hadly, E. Post-invasion demography of prehistoric humans in South America. *Nature* **2016**, doi:10.1038/nature17176.

67. De Toledo, M.B.; Bush, M.B. A mid-Holocene environmental change in Amazonian savannas. *J. Biogeogr.* **2007**, *34*, 1313–1326.

68. Blarquez, O.; Vanniere, B.; Marlon, J.; Daniau, A.; Power, M.; Brewer, S.; Bartlein, P. paleofire: An R package to analyse sedimentary charcoal records from the Global Charcoal Database to reconstruct past biomass burning. *Comput. Geosci.* **2014**, *72*, 255–261, doi:10.1016/j.cageo.2014.07.020.

69. Bush, M.; Miller, M.; De Oliveira, P.; Colinvaux, P. Two histories of environmental change and human disturbance in eastern lowland Amazonia. *Holocene* **2000**, *10*, 543–553, doi:10.1191/095968300672647521.

70. Behling, H.; da Costa, M.L. Holocene vegetational and coastal environmental changes from the Lago Crispim record in northeastern Pará State, eastern Amazonia. *Rev. Palaeobot. Palynol.* **2001**, *114*, 145–155.

71.   Behling, H.; da Costa, M.L. Holocene environmental changes from the Rio Curuá record in the Caxiuanã region, eastern Amazon Basin. *Quaternary Res.* **2000**, *53*, 369–377.

72.   Behling, H. Late Quaternary environmental changes in the Lagoa da Curuca region (eastern Amazonia, Brazil) and evidence of Podocarpus in the Amazon lowland. *Veg. Hist. Archaeobot.* **2001**, *10*, 175–183, doi:10.1007/PL00006929.

73.   Bush, M.; Silman, M.; de Toledo, M.; Listopad, C.; Gosling, W.; Williams, C.; de Oliveira, P.; Krisel, C. Holocene fire and occupation in Amazonia: records from two lake districts. *Phil. Trans. Roy. Soc. B-Biol. Sci.* **2007**, *362*, 209–218, doi:10.1098/rstb.2006.1980.

74.   Ohata, S.; Moteki, N.; Schwarz, J.; Fahey, D.; Kondo, Y. Evaluation of a Method to Measure Black Carbon Particles Suspended in Rainwater and Snow Samples. *Aerosol Sci. Technol.* **2013**, *47*, 1073–1082, doi:10.1080/02786826.2013.824067.

75.   Schwarz, J.; Gao, R.; Fahey, D.; Thomson, D.; Watts, L.; Wilson, J.; Reeves, J.; Darbeheshti, M.; Baumgardner, D.; Kok, G.; et al. Single-particle measurements of midlatitude black carbon and light-scattering aerosols from the boundary layer to the lower stratosphere. *J. Geophys. Res.-Atmos.* **2006**, *111*, doi:10.1029/2006JD007076.

76.   Adolf, C.; Wunderle, S.; Colombaroli, D.; Weber, H.; Gobet, E.; Heiri, O.; van Leeuwen, J.; Bigler, C.; Connor, S.; Galka, M.; et al. The sedimentary and remote-sensing reflection of biomass burning in Europe. *Glob. Ecol. Biogeogr.* **2018**, *27*, 199–212, doi:10.1111/geb.12682.

77.   Denevan, W.M. Estimating Amazonian Indian numbers in 1492. *Journal of Latin American Geography* **2014**, 207-221.

78.   Koch, A.; Brierley, C.; Maslin, M.M.; Lewis, S.L. Earth system impacts of the European arrival and Great Dying in the Americas after 1492. *Quaternary Sci. Rev.* **2019**, *207*, 13–36.

79.   Mann, M.E.; Zhang, Z.; Rutherford, S.; Bradley, R.S.; Hughes, M.K.; Shindell, D.; Ammann, C.; Faluvegi, G.; Ni, F. Global signatures and dynamical origins of the Little Ice Age and Medieval Climate Anomaly. *Science* **2009**, *326*, 1256–1260, doi:10.1126/science.1177303.

80.   Dull, R.A.; Nevle, R.J.; Woods, W.I.; Bird, D.K.; Avnery, S.; Denevan, W.M. The Columbian encounter and the Little Ice Age: Abrupt land use change, fire, and greenhouse forcing. *Ann. Assoc. Am. Geogr.* **2010**, *100*, 755–771.

81.   Nevle, R.; Bird, D.; Ruddiman, W.; Dull, R. Neotropical human-landscape interactions, fire, and atmospheric CO2 during European conquest. *Holocene* **2011**, *21*, 853–864, doi:10.1177/0959683611404578.

82.   Eichler, A.; Gramlich, G.; Kellerhals, T.; Tobler, L.; Schwikowski, M. Pb pollution from leaded gasoline in South America in the context of a 2000-year metallurgical history. *Sci. Adv.* **2015**, *1*, doi:10.1126/sciadv.1400196.

83.   Strosnider, W.; Lopez, F.; Nairn, R. Acid mine drainage at Cerro Rico de Potosi I: unabated high-strength discharges reflect a five century legacy of mining. *Environ. Earth Sci.* **2011**, *64*, 899–910, doi:10.1007/s12665-011-0996-x.

84.   Molina, L.; Gallardo, L.; Andrade, M.; Baumgardner, D.; Borbor-Cordova, M.; Borquez, R.; Casassa, G.; Cereceda-Balic, F.; Dawidowski, L.; Garreaud, R.; et al. Pollution and its Impacts on the South American Cryosphere. *Earths Future* **2015**, *3*, 345–369, doi:10.1002/2015EF000311.

85.   Lee, Y.H.; Lamarque, J.F.; Flanner, M.G.; Jiao, C.; Shindell, D.T.; Berntsen, T.; Bisiaux, M.M.; Cao, J.; Collins, W.J.; Curran, M.; et al. Evaluation of preindustrial to present-day black carbon and its albedo forcing from Atmospheric Chemistry and Climate Model Intercomparison Project (ACCMIP) (vol 13, pg 2607, 2013). *Atmos. Chem. Phys.* **2013**, *13*, 6553–6554, doi:10.5194/acp-13-6553-2013.

86.   Boden, T.A.; Marland, G.; Andres, R.J. *Global, Regional, and National Fossil-Fuel CO2 Emissions*; Carbon Dioxide Information Analysis Center, Oak Ridge National Laboratory, U.S. Department of Energy: Oak Ridge, TN, USA, 2011.

87.   Lasslop, G.; Coppola, A.I.; Voulgarakis, A.; Yue, C.; Veraverbeke, S. Influence of Fire on the Carbon Cycle and Climate. *Curr. Clim. Chang. Rep.* **2019**, 1-12.

88.   Chadwick, R.; Good, P.; Martin, G.; Rowell, D. Large rainfall changes consistently projected over substantial areas of tropical land. *Nature Climate Change* **2015**, doi:doi:10.1038/nclimate2805.

89.   Xu, L.; Wang, A.; Wang, D.; Wang, H. Hot Spots of Climate Extremes in the Future. *J. Geophys. Res.: Atmos.* **2019**, *0*, doi:10.1029/2018JD029980.

90. Le Page, Y.; Morton, D.; Hartin, C.; Bond-Lamberty, B.; Pereira, J.; Hurtt, G.; Asrar, G. Synergy between land use and climate change increases future fire risk in Amazon forests. *Earth Syst. Dyn.* **2017**, *8*, 1237–1246, doi:10.5194/esd-8-1237-2017.

91. Koch, D.; Schulz, M.; Kinne, S.; McNaughton, C.; Spackman, J.; Balkanski, Y.; Bauer, S.; Berntsen, T.; Bond, T.; Boucher, O.; et al. Evaluation of black carbon estimations in global aerosol models. *Atmos. Chem. Phys.* **2009**, *9*, 9001–9026.